

# Beam duct for the 1 MW neutral beam heating injector on TCV

M. Toussaint<sup>a</sup>, S. Coda<sup>a</sup>, F. Dolizy<sup>a</sup>, J. Dubray<sup>a</sup>, B. Duval<sup>a</sup>, A.N. Karpushov<sup>a</sup>, D.Keeling<sup>b</sup>, U.Siravo<sup>a</sup>  
and the TCV team<sup>a</sup>

<sup>a</sup>Ecole Polytechnique Fédérale de Lausanne (EPFL), Swiss Plasma Center (SPC), CH-1015 Lausanne, Switzerland

<sup>b</sup>Culham Center Fusion Energy, Culham Science Centre OX14 3DB Abingdon, United Kingdom

The Tokamak à Configuration Variable (TCV) has been recently equipped with a 1 MW neutral beam heating (NBH) injector [1]. Two new stainless steel ports with rectangular aperture of 170x220mm have been manufactured and installed for this purpose. The NBH injector is connected to one of them via a stainless steel port extension. The port and its extension together form the beam duct between the TCV vacuum vessel (VV) and the NBH injector.

A preliminary thermal analysis of the beam duct showed no expectation of thermal events such as overheating. Indeed, although the beam power density near the internal faces of the beam duct reaches  $\sim 10 \text{ MW/m}^2$ , the very grazing incidence angle between the beam axis and the wall was expected to lead to a maximal effective heat flux of  $\sim 350 \text{ kW/m}^2$  for a maximal duration of 2 seconds, resulting in acceptable temperature rise.

As a result, the beam duct did not include any provision for cooling. However, early in 2016 the commissioning of the NBH injector showed high overheating of the port extension, resulting in local melting and ultimately vacuum leak. This paper describes the design and analysis of an actively cooled beam duct and the status of the beam duct.

Keywords: TCV, Neutral Beam Heating, Injector, Cooling.

## 1. Introduction

The TCV has recently undergone a major upgrade including, among other systems, the installation of a 1MW NBH injector [2]. For efficient plasma heating the NBH injector required the installation of a new port with rectangular aperture of 170x220mm oriented tangentially relative to the plasma axis. Due to the severe space restrictions on TCV, this is the maximum viable port size.

The beam duct connects the NBH injector to the TCV vacuum vessel (VV). It is composed of two parts: the rectangular port which is welded to the VV and an extension for the connection to the circular NBH injector bellow, DC break and gate valve assembly (Fig. 1).

The purpose of this paper is mainly focused on the thermal behavior of the rectangular port and the extension. Indeed, the bellow, the DC break and the gate valve are not in the view line of the beam.

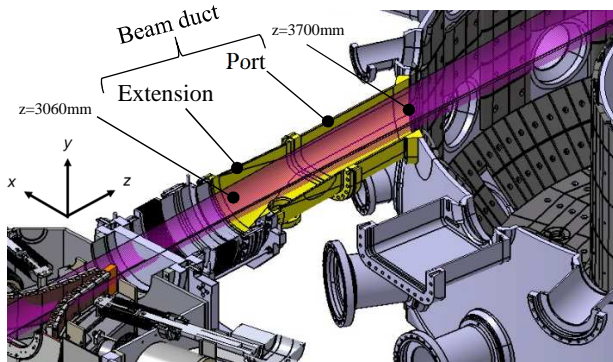


Fig. 1. Horizontal cut of the NBH injector, the beam duct and the TCV VV.

The NBH injector provides a neutral beam into the plasma for heating and current drive. For TCV operations, the NBH injector nominal regime foresees a 2-second shot at 1MW power, every 12 minutes.

The neutral beam propagation model [3] which is used for simulations has the following parameters:

- Circular grids  $\varnothing 250\text{mm}$ .
- Angular divergence along the slits (vertical direction)  $\delta\alpha_{\parallel}=12 \text{ mrad}$ .
- Angular divergence across the slits (horizontal direction)  $\delta\alpha_{\perp}=20 \text{ mrad}$ .
- Optimal focal distance of the grid system  $F=3600 \text{ mm}$ .

The beam power density profile can be approximated by a Gaussian (Equation 1) and is evolving along the beam axis  $z$  (Fig. 2 and Fig. 3).

$$P_{x,y} = P_{max} \cdot e^{-\left(\frac{x}{\alpha_x}\right)^2 - \left(\frac{y}{\alpha_y}\right)^2} \quad (1)$$

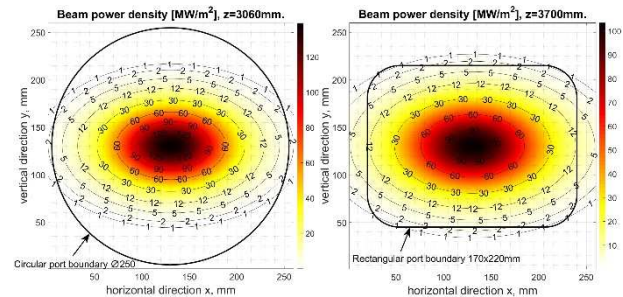


Fig. 2. Beam power density profile at  $z=3060\text{mm}$ .

Fig. 3. Beam power density profile at  $z=3700\text{mm}$ .

## 2. Original beam duct

The preliminary design assessments assumed a stainless steel (EN 1.4429) duct with internal faces parallel to the beam axis, receiving an effective power flux of  $\sim 350 \text{ kW/m}^2$ . The expected localized maximal surface temperature after a 2 sec shot was  $\sim 550^\circ\text{C}$  (Fig. 7, value at  $z=3700\text{mm}$ ). Thus, the original beam duct did not include any provisions for thermal protection or active cooling.

However, the final design included tangential ports (Fig.4) for prospective diagnostics and/or additional differential pumping of the duct. Moreover, with its circular to rectangular geometry, the extension intrinsically features faces that are not parallel to the beam axis. Therefore, including those design details, the resulting effective heat flux reached  $\sim 3.6\text{-}4.8 \text{ MW/m}^2$  in the worst region (beam incidence close to  $45^\circ$ , Fig.4). After several shots at nominal regime, overheating and local melting of the port extension occurred, resulting in vacuum leak.

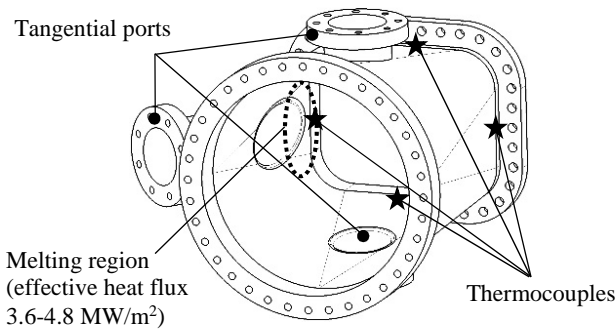


Fig. 4. Final design of the original port extension.

To explain the observed damages, a FEA thermal transient (Fig.5) has been performed with the original geometry. The settings of the analysis are as follows:

- ANSYS transient module [4].
- Simplified 3D model (controlled surface contacts).
- Heat flux imported as a 3D distribution from MATLAB model with angle of incidence factor on internal faces.
- 2 sec. shot at full (1MW) beam power.
- Thermal radiation neglected, emissivity coefficient of duct (electro-polished stainless steel) being  $< 0.1$ .

The result shows an unacceptable localized temperature of over  $4000^\circ\text{C}$  after a 2 seconds shot at NBH nominal regime (Fig.5), confirming the observation of local melting.

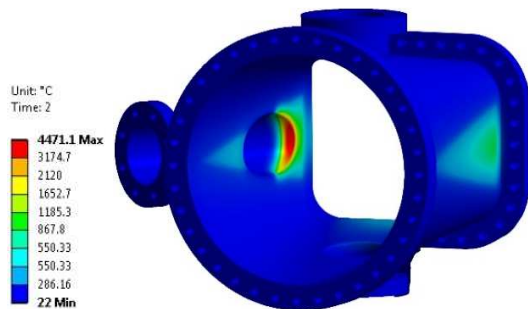


Fig. 5. Temperature at  $t=2$  seconds.

## 3. Current beam duct

The hole has been repaired and the damaged tangential port moved to the top side, where the peak power density is  $\sim 4$  times smaller than on the lateral side. Thermocouples have been installed on the 4 external faces of the extension (Fig. 4). Measurements performed (Fig. 6) show that the elevation temperature evaluated by extrapolation on the inner faces of the extension was  $\sim 500^\circ\text{C}$  per shot at NBH nominal regime.

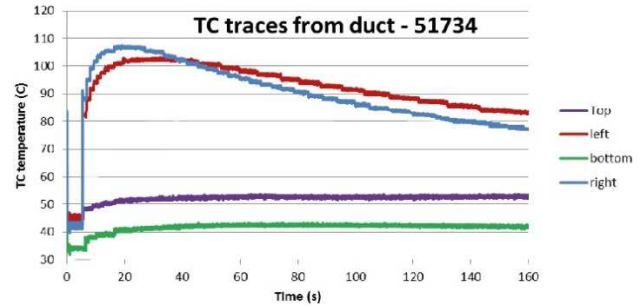


Fig. 6. Thermocouples traces, external surface of extension.

To compare the measurements, a FEA thermal transient has been performed with the current geometry (Fig. 7 and 8). In addition to the previous analysis settings, cooling is taken into consideration as follows:

- Port extension with natural convective cooling of  $5 \text{ W/m}^2\text{K}$  (conduction at both extremities very limited by low surface contact of vacuum seals).
- Port itself cooled by conduction with the  $20^\circ\text{C}$  VV at one extremity (thermal insulation layers prevent any natural convection on the port).

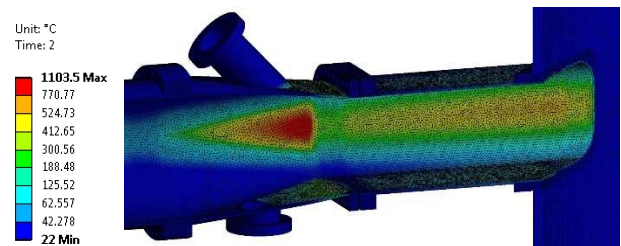


Fig. 7. Temperature at  $t=2$  seconds.

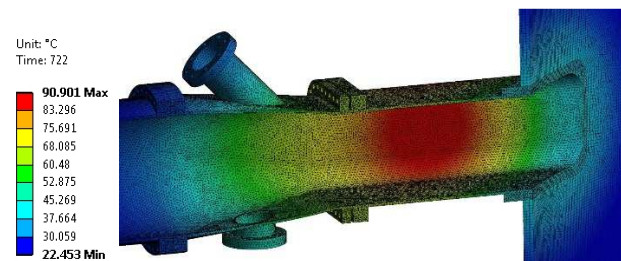


Fig. 8. Temperature at  $t=12$  minutes.

Both measures and analytical analysis show that melt damage on internal faces may still occur and temperature 12 minutes after a shot at NBH nominal regime is still  $\sim 90^\circ\text{C}$  in the port and  $\sim 70^\circ\text{C}$  in the extension. Therefore, a hot spot protection of the internal faces and an active cooling have to be installed to allow the NBH operation at nominal regime.

## 4. New beam duct

### 4.1 First design option

The first design option employs a layer of tiles (Fig.9) acting as a hot spots shield for the most exposed internal faces. The tiles are mechanically and thermally connected to an actively cooled stainless steel flange using M4 screws every 30mm intervals (Fig.10). The contact faces have a final milling operation to optimize the flatness. Graphite conduction sheets of 0.07mm thickness (easily deformable at low contact pressures, with thermal conductivity 1000W/mK) are used as interlayer to improve the thermal contact. For sputtering issues (plasma pollution), graphite is preferred for the tiles due to its low atomic mass.

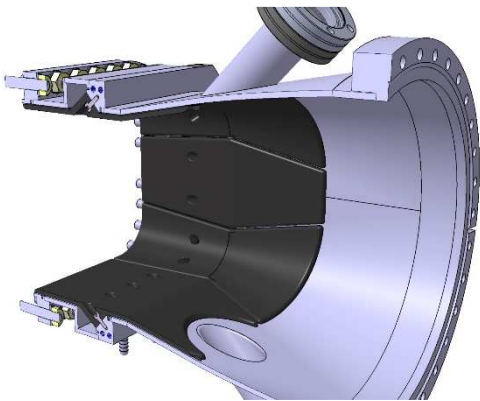


Fig. 9. General view of the thermal protection tiles.

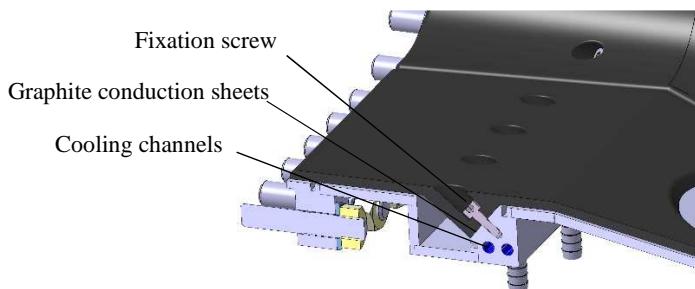


Fig. 10. Detailed view of the tile fixation and cooling.

A FEA thermal transient has been performed with the following settings:

- ANSYS transient module [4].
- Simplified 3D model (controlled surface contacts).
- Heat flux imported as a 3D distribution from MATLAB model with angle of incidence factor on internal faces.
- Tiles in graphite, tungsten or copper.
- 2 sec. shot at full (1MW) beam power.
- Thermal radiation included, emissivity coefficient of 0.7 for graphite, 0.3 for tungsten and neglected for copper (<0.1) (conservative values are used).
- 720sec (12 min) of active cooling inside the cooling channels of the flange. Heat transfer coefficient of 10'000 W/m<sup>2</sup>K has been estimated ( $\Delta T$  of the cooling water fixed to 30°C).

- Port extension with natural convective cooling of 5 W/m<sup>2</sup>K (conduction at both extremities very limited by low surface contact of vacuum seals).
- Port itself cooled by conduction with the 20°C VV at one extremity (thermal insulation layers prevent any natural convection).

The maximal surface temperature (Fig. 11) after a 2sec NBH shot at nominal regime reached the following values for different tile materials:

- ~ 4400°C for graphite, not acceptable.
- ~ 2500°C for tungsten, acceptable.
- ~ 1650°C for copper, not acceptable.

This considerable temperature increase occurs only on the nose of the tiles which are exposed near-perpendicularly to the beam (solution avoiding the nose is described in the next section). Thermal expansion has to be considered at such high temperatures. Nevertheless, the temperature never exceed 300°C in the fixation region, giving a lateral expansion (for 30mm) of ~0.05mm for graphite, 0.04mm for tungsten and 0.14 for copper, which is rendered possible with the passing holes. Thermal expansion of the thickness of the tiles generates a compression stress of ~25 MPa for graphite (acceptable), 530 MPa for tungsten (not acceptable) and 600 MPa for copper (not acceptable). The inter-shot cooling system works well for tungsten and copper tiles but is not sufficient for graphite due to lower thermal conductivity (Fig. 12). Independently of the tile materials, the rectangular port attached to the TCV VV must also be cooled (which is, as yet, not foreseen).

In conclusion, this design option is not suitable (too high temperatures for graphite or copper and too much stresses due to the thermal expansion for tungsten and copper). The next chapter describes a second design option.

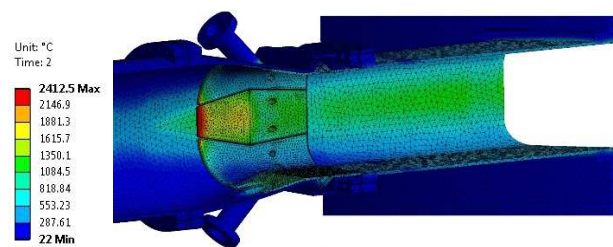


Fig. 11. Temperature at t= 2 seconds, tungsten tiles.

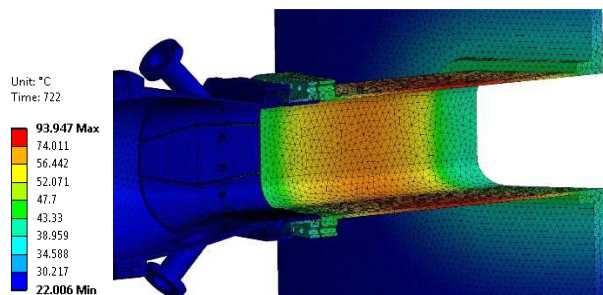


Fig. 12. Temperature at t= 12 minutes, tungsten tiles.

## 4.2 Second design option

A second, improved conceptual design is proposed. It is composed of an insert, integrated inside the beam duct (Fig. 13). No surfaces intercept the beam near-perpendicularly, reducing the maximal heat flux on the internal faces by a factor 3.

The insert is attached to an actively cooled stainless steel flange to permit cooling between shots (cooling not represented on figure 13). Its width is limited by the proximity to toroidal field coils casing (Fig. 13). As the 3D model has been created only for a preliminary thermal analysis, the insert does not show any holes for tangential ports integration, but they would be added if this option is chosen. The preferred material for the insert is graphite, due to its low atomic mass.

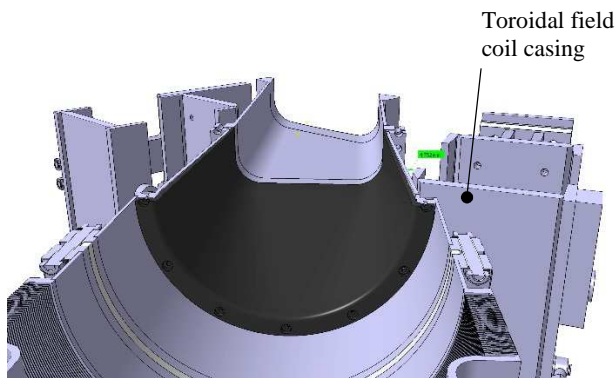


Fig. 13. Back view, horizontally cut, of the thermal protection insert.

A FEA thermal transient has been performed (Fig.14) for an insert made of graphite, tungsten or copper. The 720 sec (12min) of cooling phase is not considered as it is not the critical issue. The same settings than in chapter 4.1 are used, except for radiation which is neglected (radiation does not play a significant role for such temperatures, conservative approach). The maximal surface temperature after a 2sec NBH shot at nominal regime reached the following values for different insert materials:

- ~ 2900°C for graphite insert, not acceptable.
- ~ 1500°C for tungsten insert, acceptable.
- ~ 1000°C for copper insert, not acceptable.

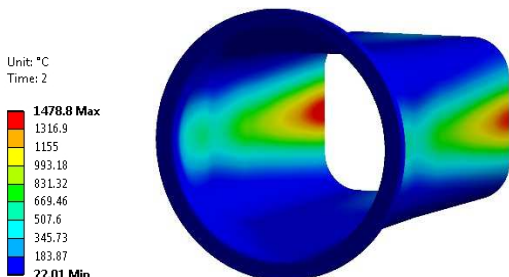


Fig. 14. Temperature at t= 2 seconds, tungsten insert.

The temperature decreases significantly with this second design option. The use of graphite, however, is too risky considering the possibility of beam misalignments for example.

## 5. Conclusions and outlook

According to the FEA thermal transient which have been performed, only a design with tungsten could withstand the NBH nominal regime. Indeed, with the geometry and size restrictions due to TCV configuration, any solution strongly depends on the material of the thermal shield.

The graphite is by far preferred for sputtering issues (due to its low atomic mass) and compatibility with TCV graphite first wall, but is still problematic from a thermal viewpoint, even though the second design option shows a significant improvement in terms of temperature.

Active cooling is required between shots to lower the temperature in the extension and in the port. The port is currently thermally insulated to improve its baking. The removal of this insulation is required in order to install a cooling device. Investigations have to be carried out concerning the thermal behavior of the port without the insulation during the TCV bake-out.

The NBH injector source is currently undergoing maintenance and improvement (lower divergence and optimization of focal length). After this operation, the beam properties may change.

The thermal protection of the beam duct being challenging to set up and temperatures for the current stainless steel beam duct or for the graphite insert being close to acceptable values, the decision was taken to wait until the new injector beam is measured and numerically reconstructed. A decision to either keep the current stainless steel beam duct or install a thermal shield (preferably made of graphite or possibly of tungsten) will be made on a more quantitative basis.

An apparatus to measure the heat flux at the beam duct position and options for cooling of the rectangular port are therefore the next steps to be investigated, designed, manufactured and installed for solving the problem of the beam duct overheating.

## References

- [1] A. Fasoli for the TCV team, TCV Heating and In-Vessel Upgrades for Addressing DEMO Physics Issues, Nuclear Fusion **55** (2015) 043006 .
- [2] A.N. Karpushov et al., Neutral beam heating on the TCV tokamak, this conference.
- [3] Akhmetov,T.D.; Davydenko,V.I.; Ivanov,A.A.; **Model of neutral-beam propagation in a duct with scrapers**; IEEE Trans. Plasma Sci. (USA), v.36, n.4, Aug. 2008, p.1545-51; [DOI:10.1109/TPS.2008.917951](https://doi.org/10.1109/TPS.2008.917951)
- [4] [www.ansys.com](http://www.ansys.com)